High-Fidelity, High-Performance Full-Wave Computational Algorithms for Intra-System EMI Analysis of IC and Electronics

Shen Lin, Hong-Wei Gao and Zhen Peng
University of New Mexico
Albuquerque, NM 87131-0001, U.S.A.
Telephone: (505) 277–1904
Email: pengz@unm.edu

***Abstract*—The objective of this work is to investigate high-resolution, high-performance full-wave field solvers towards scalable electromagnetic simulations of product-level ICs and electronics. The emphasis is put on advancing parallel algorithms that are provably scalable, facilitating a design-through-analysis paradigm, and enabling concurrent multi-scale modeling and computation. The capability and benefits of the algorithms are validated and illustrated through complex 3D IC and electronics applications.**

I. Introduction

Emerging integrated circuit (IC) and package systems, such as system-on-a-chip (SoC) s system-on-package (SoP), system-in-package (SiP), antenna-in-package (AiP) and package-on-package (PoP) have emerged as an efficient and powerful solution for realizing complex electronic products with smaller size, increased functionality and lower cost. The proliferation of such 3D IC and packaging technologies [1] is opening up tremendous possibilities for continuing extending Moore's Law in designing complex systems with applications ranging from mobile devices, aerospace electronics, computing and communications, automotive and medical systems. However, much potential is not fully exploited yet due to a lack of comprehensive and high fidelity modeling and simulation tools in analyzing, designing and verifying increasingly complex designs and integration.

IC designers and researchers have initiated the transition from traditional circuit-based simulation to electromagnetic (EM) field-based modeling methodology to achieve the necessary solution accuracy at higher frequencies [2]–[6]. However, the growing sophistication in IC design presents significant computational challenges in existing full-wave field solvers in terms of desired accuracy, efficiency and scalable parallelism. Furthermore, to accurately predict in-situ IC performance, intra-system interactions of 3D interconnects, packages, printed circuit boards (PCBs) and systems must be considered simultaneously. One major computational challenge is that individual sub-systems often exhibit vast differences in the aspect ratios (ratio of wavelength to feature size). Even with state-of-the-art full wave approaches, the computational resources required for such large multi-scale problems are prohibitively expensive. Consequently, there is an urgent need for rigorous, hierarchical multi-scale simulation methods to analyze the performance of these in-situ package systems in realistic circumstances.

This work aims to investigate first-principles analysis and verification tools for complex electronic systems ranging from circuit, package, board and system levels. A novel augmented multi-region multi-scale domain decomposition (DD) method is proposed. It introduces a simulation flow that breaks the entire electronic system into many small sub-systems (or sub-domains), and applies the best solution strategy to solve for each sub-system. To facilitate this electrical partitioning of complex systems, a well-conditioned multi-trace integral equation formulation is introduced on the surfaces of individual sub-systems. Subsequently, a Schwarz iterative process is used to adjust boundary conditions for sub-system problems until the solution converges. To further improve the efficiency of this work, we exploit the rank deficiency property exhibited in the interaction matrices between sub-systems and construct a hierarchical skeletonization-based compressed system. The interactions between sub-systems are computed using selected skeletons, and the Schwarz iteration is performed on the compressed skeleton system. Numerical results show that the method is promising to simultaneously simulate heterogeneous sub-systems exhibiting vast differences in the aspect ratios, and provides concurrent resolution of multiple scales in the computational domain.

II. Technical Approach

The proposed scheme follows a hierarchical multi-level domain partitioning strategy. The electronic system is firstly divided into case, board and package sub-systems. Each sub-system may be further decomposed into sub-domains, where local repetitions and periodicities can be exploited. The domain partitioning between sub-systems does not need to be shape-conforming, and the discretizations do not require to be matching. Thus, model preparation and mesh generation can be performed concurrently and are naturally parallelizable.

To facilitate this space partitioning of complex systems, Huygen's equivalent sources (i.e. electric and magnetic current sources) are introduced on the surfaces of individual sub-systems. Subsequently, these sub-systems are coupled to one another via the representation formula (distant sub-systems) and transmission conditions (adjacent sub-systems) [7]. An Schwarz iterative process is used to adjust boundary conditions for sub-system problems until the solution converges. It is expected to be a suitable paradigm not only for the high-fidelity system level simulation that is accurate across the full scale

range, but also for the integration of state-of-the-art solvers from each sub-system into a powerful solution suite. Thus, the method is denoted by the multi-region multi-solver domain decomposition method (MR-MS-DDM).

To illustrate, we consider the case that the electronic system is decomposed into N sub-systems, Ω_m, $m = 0, 1, \cdots N$. Through this decomposition, we introduce two pairs of trace data on each sub-system surface, $\partial\Omega_m$. These traces are the Neumann trace $\mathbf{j}_m$ and Dirichlet trace $\mathbf{e}_m$, defined by:

$$\mathbf{j}_m = \frac{1}{ik_0}\hat{\mathbf{n}}_m \times \frac{1}{\mu_{rm}}\nabla \times \mathbf{E}_m \tag{1}$$

$$\mathbf{e}_m = \hat{\mathbf{n}}_m \times \mathbf{E}_m \times \hat{\mathbf{n}}_m \tag{2}$$

Next, a general Schwarz algorithm [8] for the decomposed problem can be described as follows: Solve iteratively for iteration $p = 1, 2, \cdots$ the following sub-system problems

$$\mathcal{G}_m\left(\mathbf{e}_m^p, \mathbf{j}_m^p\right) = \mathbf{y}_m^{\text{inc}} \qquad \text{on } \partial\Omega_m \tag{3}$$

$$\mathcal{B}_{mn}\left(\mathbf{e}_m^p, \mathbf{j}_m^p\right) = \mathcal{B}_{mn}\left(\mathbf{e}_n^{p-1}, -\mathbf{j}_n^{p-1}\right) \quad \text{on } \Gamma_{mn}, \forall\Gamma_{mn} \in \Gamma_m \tag{4}$$

where $\mathcal{G}_m$ denotes the full-wave field solver for sub-system Ω_m, and Γ_{mn} is the interface between adjacent sub-systems Ω_m and Ω_n. $\mathcal{B}_{mn}$ usually consists of tangential pseudo-differential operators defined at the interface Γ_{mn}. Equation (4) denotes the TC used to couple the Dirichlet and Neumann traces at the interfaces. For instance, when the first (1^{st}) order Robin-type TC [9]–[11] is employed, we have $\mathcal{B}_{mn}\left(\mathbf{e}, \mathbf{j}\right) := \mathbf{e} - \bar{\eta}_m\mathbf{j}$. In a recent work [12]–[14], we propose a second (2^{nd}) order TC:

$$\begin{aligned}\mathcal{B}_{mn}\left(\mathbf{e}, \mathbf{j}\right) :=& \left(\mathcal{I} + \kappa_1\nabla_\tau \times \nabla_\tau \times + \kappa_2\nabla_\tau\nabla_\tau\cdot\right)\mathbf{e} \\ &- \left(\mathcal{I} + \kappa_3\nabla_\tau \times \nabla_\tau \times + \kappa_4\nabla_\tau\nabla_\tau\cdot\right)\bar{\eta}\mathbf{j}\end{aligned} \tag{5}$$

at the interface between two different materials, where $\nabla_\tau \times \nabla_\tau\times$ and $\nabla_\tau\nabla_\tau\cdot$ are 2^{nd} order tangential derivatives and τ denotes the tangential direction. κ_1, κ_2, κ_3, and κ_4 are the parameters that can be chosen to obtain rapidly converging algorithms.

To further improve the capability and efficiency of this work, we construct a hierarchical skeleton-based compressed system to reduce the computational complexity. It exploits the rank deficiency property exhibited in the interaction matrices between sub-systems. We first employ the multi-level skeletonization [15] to construct effective basis functions, the so-called skeletons, from Huygen's equivalent sources associated with individual sub-systems. This skeletonization process is rigorous, error controllable, and can be achieved locally per sub-system and in parallel. Subsequently, the interactions between sub-systems will be computed using selected skeletons, and the DD iteration will be performed on the compressed skeleton system.

To illustrate, we consider the following linear system after domain decomposition (for simplicity, two sub-systems are considered):

$$\begin{bmatrix} \mathcal{A}_1 & \mathcal{C}_{12} \\ \mathcal{C}_{21} & \mathcal{A}_2 \end{bmatrix}\begin{bmatrix} \mathbf{u}_1 \\ \mathbf{u}_2 \end{bmatrix} = \begin{bmatrix} \mathbf{y}_1 \\ \mathbf{y}_2 \end{bmatrix} \tag{6}$$

In (6), $\mathcal{A}_m$ denotes the sub-domain matrix, and $\mathcal{C}_{mn}$ is the coupling matrix. The matrix equation (6) is solved with a preconditioned Krylov subspace method with an additive Schwarz preconditioner [16]. The preconditioned system matrix equation with respect to surface unknowns can be written as:

$$\begin{bmatrix} \mathcal{I} & \bar{\mathcal{R}}_1\mathcal{A}_1^{-1}\bar{\mathcal{R}}_1^T\bar{\mathcal{C}}_{12} \\ \bar{\mathcal{R}}_2\mathcal{A}_2^{-1}\bar{\mathcal{R}}_2^T\bar{\mathcal{C}}_{21} & \mathcal{I} \end{bmatrix}\begin{bmatrix} \bar{\mathbf{u}}_1 \\ \bar{\mathbf{u}}_2 \end{bmatrix} = \begin{bmatrix} \bar{\mathbf{y}}_1 \\ \bar{\mathbf{y}}_2 \end{bmatrix} \tag{7}$$

where we have introduced a simple restriction operator $\bar{\mathcal{R}}_m$ for the coefficient vector $\mathbf{u}_m$. We have $\bar{\mathbf{u}}_m = \bar{\mathcal{R}}_m\mathbf{u}_m$ and $\bar{\mathcal{C}}_{mn} = \bar{\mathcal{R}}_m^T\mathcal{C}_{mn}\bar{\mathcal{R}}_n$.

Next, we apply the multi-level skeletonization to the coupling matrix, which can be expressed as: $\bar{\mathcal{C}}_{mn} = \mathcal{V}_m\mathcal{S}_{mn}\mathcal{V}_n^T$. After some algebraic manipulations, the reduced system equation in terms of only the skeletoned surface unknowns can be written as:

$$\begin{bmatrix} \mathcal{I} & \mathcal{V}_1^T\bar{\mathcal{R}}_1\mathcal{A}_1^{-1}\bar{\mathcal{R}}_1^T\bar{\mathcal{V}}_1\mathcal{S}_{12} \\ \mathcal{V}_2^T\bar{\mathcal{R}}_2\mathcal{A}_2^{-1}\bar{\mathcal{R}}_2^T\bar{\mathcal{V}}_2\mathcal{S}_{21} & \mathcal{I} \end{bmatrix}\begin{bmatrix} \bar{\bar{\mathbf{u}}}_1 \\ \bar{\bar{\mathbf{u}}}_2 \end{bmatrix} = \begin{bmatrix} \bar{\bar{\mathbf{y}}}_1 \\ \bar{\bar{\mathbf{y}}}_2 \end{bmatrix} \tag{8}$$

where $\bar{\bar{\mathbf{u}}}_m = \mathcal{V}_m^T\bar{\mathbf{u}}_m$. Once the skeletoned surface unknowns $\bar{\bar{\mathbf{u}}}_m, m = 1, 2$, are computed, the solution for each sub-domain can be recovered through backward substitutions.

In summary, instead of directly applying Schwarz DD scheme to the original full-scale system with N degrees of freedom (DOFs), we construct a coarse-grained compressed system to reduce the DD matrix dimension from $\mathcal{O}(N)$ to $\mathcal{O}(M)$, where M is the number of skeletoned surface unknowns. A dramatic reduction in computational complexity is expected since M will be a much smaller number than N regarding to 3D IC applications of interest. Finally, based on the proposed algorithms, we have developed a hybrid MPI/OpenMP parallel implementation of the proposed work on shared and distributed memory supercomputers.

III. Numerical Results

We first consider a validation example by simulating two monopole antennas mounted inside a closed surface PEC cavity. The computational domain is decomposed into three regions: 1) interior cavity region; 2) long monopole; and 3) short monopole, as shown in Fig. 1. The geometry of each monopole is also illustrated. After decomposition, the multi-trace boundary integral equation method [14] is used to discretize the cavity sub-domain Ω_1, and the finite element method is employed to discretize the antenna sub-domains Ω_2 and Ω_3. In the simulation, we excite the short monopole and use the long monopole as the receiving antenna. The computed S_{11} and S_{12} with respect to different operating frequencies are shown in Fig. 2. The measurement results conducted in Applied EM Group at University of New Mexico (UNM) are also given in Fig. 2. We observed an excellent agreement between the results obtained by computation and measurement. Finally, the surface electric current distributions at two operating frequencies, $f = 831.8$MHz and $f = 833.2$MHz, are plotted in Fig. 3. One is non-resonant frequency with $\mathrm{S}_{11} = 0.9838$ and $\mathrm{S}_{12} = 0.0761$. The other one is resonant frequency with $\mathrm{S}_{11} = 0.635$ and $\mathrm{S}_{12} = 0.562$.

The second numerical example is a complex electronic system shown in Fig. 4, in which a product-level IBM package [17] is integrated on a generic printed circuit board. The printed circuit board, along with a monopole antenna and a mode stir, is located inside a complicated perfect electric

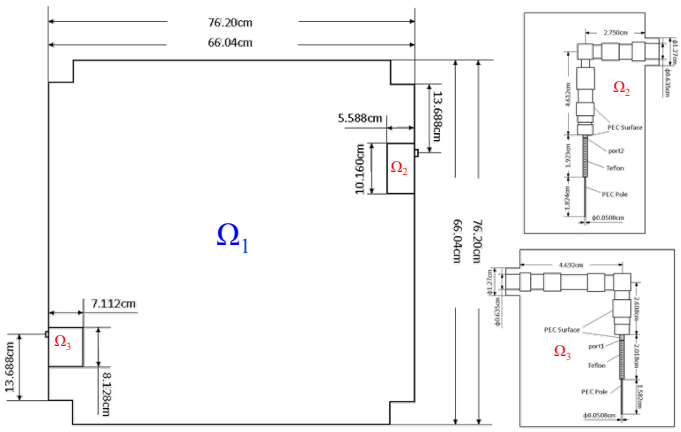

Fig. 1. Configuration of the validation example and geometry of the antennas.

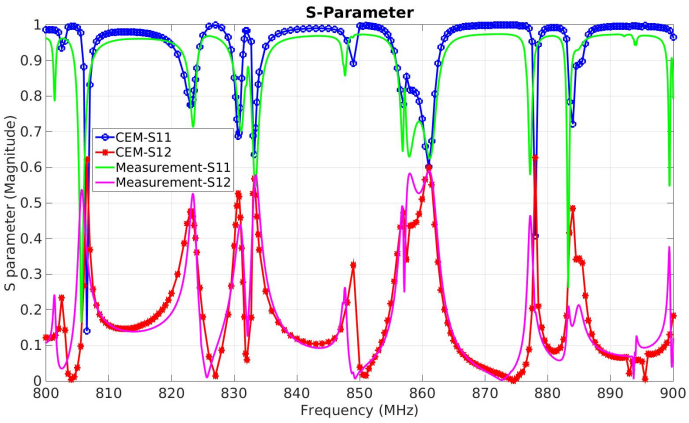

Fig. 2. Comparison of S-parameters obtained by computation and measurement.

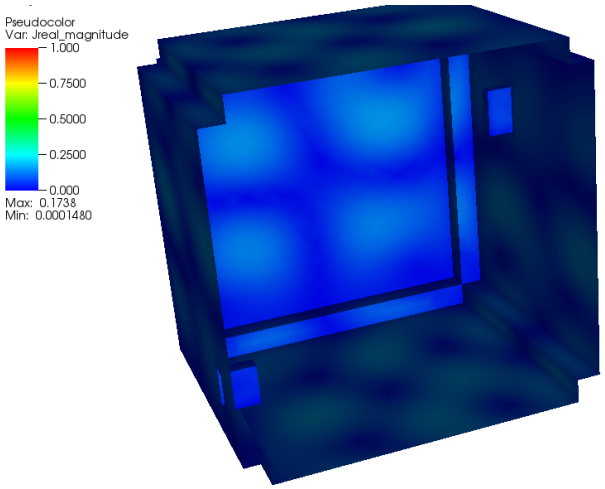

(a) $f = 831.8$MHz

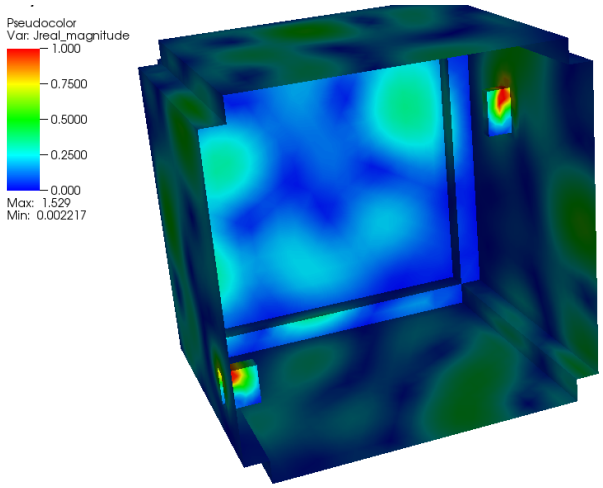

(b) $f = 833.2$MHz

Fig. 3. Surface electric current at non-resonant and resonant frequencies

conducting (PEC) cavity. As illustrated in Fig. 4, individual sub-systems exhibit vast differences in the aspect ratios (ratio of wavelength to feature size).

Following the proposed hierarchical domain partitioning strategy, the electronic system is firstly divided into cavity, antenna, mode stir, board and package sub-systems. Each sub-system is further decomposed into sub-domains based on the number of processors available and the local memory each processor can access. Next, the well-conditioned multi-trace boundary integral equation solver [14] is applied to electrically large cavity and mode stir sub-domains. The finite element DD solver [18] is applied to electrically small but geometrically complicated sub-domains, board, package, and antenna, respectively. Due to the complexities of the entire system, it results in 75 millions DOFs and a total number of 624 sub-domains. After skeletonization, we obtain a coarse-grained compressed DD system with a total number of 5.4 millions surface DOFs.

The simulation requires 8 iterations to reach a relative residual 10^{-2}. The computation takes 7 hour per iteration. The surface current and EM field distributions with respect to antenna radiation at 10GHz are given in Fig. 5. The results show that the method is promising to simultaneously simulate heterogeneous sub-systems exhibiting vast differences in the aspect ratios, and provides concurrent resolution of multiple scales in the computational domain. The simulation is conducted at UNM Center for Advanced Research Computing.

IV. Conclusion

The objective of this work is to investigate high-resolution and high-performance full-wave computational methods for the intra-system EMI analysis of in-situ IC and packages. The novelties and key technical approaches of the proposed work include: (**i**) an optimized geometry-based DD method to conquer the geometric complexity of physical domain, which leads to quasi-optimal convergence that is provably scalable for multi-scale objects. Moreover, it results in parallel and scalable computational algorithms to reduce the time complexity via high performance computing facilities; (**ii**) a hierarchical multi-scale simulator for high-definition IC package systems, where an augmented multi-region multi-solver method via skeletonization is proposed for efficient multi-scale modeling. The capability and benefits of the algorithms are explored and illustrated through several product-level IC and electronics applications.

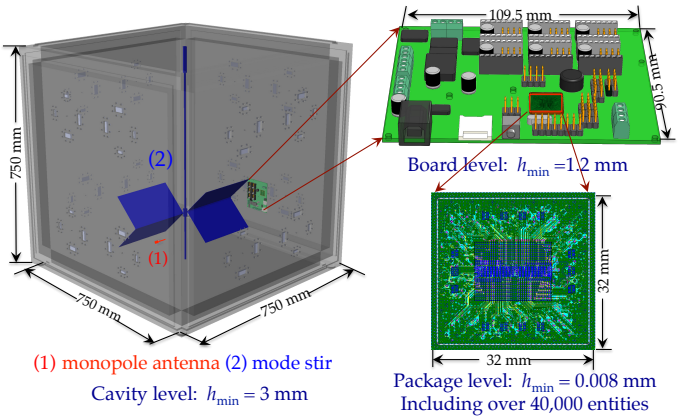

Fig. 4. A complex electronic system from case, board to package level.

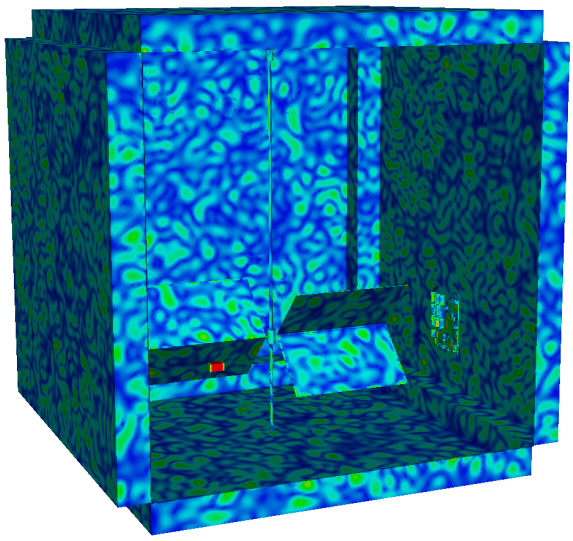

Fig. 5. Surface electric current on the complex electronic system using the augmented MR-MS-DD method

ACKNOWLEDGMENT

The work is supported by AFOSR COE: Science of Electronics in Extreme Electromagnetic Environments, Grant FA9550-15-1-0171. The authors would like to thank Ms. Ghadeh Hadi, Dr. Sameer Hemmady and Dr. Edl Schamiloglu in Applied Electromagnetics Group at University of New Mexico for the experiment and measurement results for the validation example.

REFERENCES

[1] F. Carson, Y. C. Kim, and I. S. Yoon, "3-d stacked package technology and trends," *Proc. IEEE*, vol. 97, pp. 31–42, Jan 2009.

[2] J.-M. J. A.E. Yilmaz and E. Michielssen, "A TDIE-based asynchronous electromagnetic-circuit simulator," *IEEE Microwave Wireless Compon. Lett.*, vol. 16, no. 3, pp. 122–124, 2006.

[3] K. Hollaus, O. Biro, P. Caldera, G. Matzenauer, G. Paoli, and G. Pli-eschnegger, "Simulation of crosstalk on printed circuit boards by FDTD, FEM, and a circuit model," *IEEE Trans. Magn.*, vol. 44, pp. 1486–1489, June 2008.

[4] F. Bilotti, S. Lauro, A. Toscano, and L. Vegni, "Efficient modeling of the crosstalk between two coupled microstrip lines over nonconventional materials using an hybrid technique," *IEEE Trans. Magn.*, vol. 44, pp. 1482–1485, June 2008.

[5] C. Buccella, M. Feliziani, and G. Manzi, "Three-dimensional FEM approach to model twisted wire pair cables," in *12th Biennial IEEE Conference on Electromagnetic Field Computation, 2006*, pp. 384–384, 2006.

[6] R. Wang and J.-M. Jin, "A symmetric electromagnetic-circuit simulator based on the extended time-domain finite element method," *IEEE Trans. Microwave Theory Tech.*, vol. 56, pp. 2875–2884, Dec 2008.

[7] Z. Peng, K.-H. Lim, and J.-F. Lee, "Non-conformal domain decomposition methods for solving large multi-scale electromagnetic scattering problems," *Proceedings of IEEE*, vol. 101, no. 2, pp. 298–319, 2013.

[8] A. Toselli and O. Widlund, *Domain Decomposition Methods–Algorithms and Theory*. Berlin: Springer, 2005.

[9] Z. Peng, V. Rawat, and J.-F. Lee, "One way domain decomposition method with second order transmission conditions for solving electromagnetic wave problems," *J. Comput. Phys.*, vol. 229, pp. 1181–1197, 2010.

[10] K. Zhao, V. Rawat, S.-C. Lee, and J.-F. Lee, "A domain decomposition method with nonconformal meshes for finite periodic and semi-periodic structures," *IEEE Trans. Antennas Propagat.*, vol. 55, pp. 2559–2570, Sept. 2007.

[11] Z. Peng, K.-H. Lim, and J.-F. Lee, "Computations of electromagnetic wave scattering from penetrable composite targets using a surface integral equation method with multiple traces," *IEEE Trans. Antennas Propagat.*, vol. 61, no. 1, pp. 256–269, 2013.

[12] Z. Peng, K.-H. Lim, and J.-F. Lee, "A boundary integral equation domain decomposition method for electromagnetic scattering from large and deep cavities," *J. Comput. Phys.*, vol. 280, no. 1, pp. 626–642, 2015.

[13] V. Dolean, M. J. Gander, S. Lanteri, J.-F. Lee, and Z. Peng, "Effective transmission conditions for domain decomposition methods applied to the time-harmonic curl-curl Maxwell's equations," *J. Comput. Phys.*, vol. 280, pp. 232–247, Jan. 2015.

[14] Z. Peng, "A novel multitrace boundary integral equation formulation for electromagnetic cavity scattering problems," *IEEE Trans. Antennas Propagat.*, vol. 63, pp. 4446–4457, Oct 2015.

[15] J.-G. Wei, Z. Peng, and J.-F. Lee, "Multi-scale electromagnetic computations using a hierarchical multi-level fast multipole algorithm," *Radio Science*, vol. 49, no. 11, pp. 1022–1040, 2014.

[16] Z. Peng and J.-F. Lee, "A scalable non-overlapping and non-conformal domain decomposition method for solving time-harmonic Maxwell equations in $\mathbb{R}^3$," *SIAM J. Sci. Comput.*, vol. 34, no. 3, pp. A1266–A1295, 2012.

[17] B. Krauter, M. Beattie, D. Widiger, H.-M. Huang, J. Choi, and Y. Zhan, "Parallelized full package signal integrity analysis using spatially distributed 3D circuit models," *IEEE Conf. Elect. Perform. Electron. Packag. (EPEP)*, pp. 303–306, Oct 2006.

[18] Y. Shao, Z. Peng, and J.-F. Lee, "Full-wave real-life 3-D package signal integrity analysis using nonconformal domain decomposition method," *IEEE Trans. Microwave Theory Tech.*, vol. 59, pp. 230–241, Feb 2011.